catalysts

MDPI

Article

X-Ray Emissions from Hydrogen Rydberg Matter Detected Using Timepix3 CdTe Detector †

Sindre Andre Zeiner-Gundersen * and Sveinn Olafsson

Science Institute, University of Iceland, Dunhaga 3, 107 Reykjavik, Iceland; sveinol@hi.is
* Correspondence: saz2@hi.is; Tel.: +47-906-85-000
† Supported by the Nordic Nuclear Energy Corporation, Norwegian Research Council, University of Iceland and Norront AS.

Abstract: This study investigates the X-ray emissions from Hydrogen Rydberg Matter (HRM) using a state of-the-art Timepix3 detector with a Cadmium Telluride (CdTe) sensor, which offers imaging operation. The experimental setup featured an ultra-high vacuum (UHV) chamber containing potassium-doped iron oxide catalytic source, exposed to hydrogen or deuterium gas flowing through the source. A 1064 nm pulsed YAG laser was used to stimulate the HRM. The Timepix detector was calibrated with Cs-137 662 keV and 21 keV source. Results show a prominent emission peak in the 25–50 keV range, with significant contributions at 406 keV identified through aluminum foil attenuation experiments. These findings advance our understanding of radiation phenomena in hydrogen-loaded systems and suggest new avenues for exploring the unique emissions from HRM, potentially impacting material science and catalysis.

Keywords: Hydrogen Rydberg Matter; catalyst; x-ray emission; hydrogenation

check for updates

Academic Editor: Sónia Carabineiro

Received: 18 April 2025
Revised: 13 May 2025
Accepted: 19 May 2025
Published: 26 May 2025

Citation: Zeiner-Gundersen, S.A.; Olafsson, S. X-Ray Emissions from Hydrogen Rydberg Matter Detected Using Timepix3 CdTe Detector. *Catalysts* **2025**, *15*, 526. https://doi.org/10.3390/catal15060526

Copyright: © 2025 by the authors. Licensee MDPI, Basel, Switzerland. This article is an open access article distributed under the terms and conditions of the Creative Commons Attribution (CC BY) license (https://creativecommons.org/licenses/by/4.0/).

1. Introduction

Hydrogen Rydberg Matter (HRM) has emerged as a subject of significant scientific interest due to its unique properties and potential applications in various fields, including nuclear physics, catalysis, and material science. One of the intriguing aspects of HRM is its emission of radiation during hydrogen flow through specific catalysts. Previous studies have reported spontaneous radiation emissions from an iron oxide catalyst doped with potassium (Fe_2O_3: K), commonly used in the production of styrene [1]. These emissions have been primarily observed as intermittent X-ray bursts, a finding that challenges earlier hypotheses suggesting the presence of muon radiation [2]. In the context of catalysis, understanding these emissions is crucial as they can reveal how hydrogen interacts with the catalyst surface, influencing processes like hydrogenation, which are central to industrial applications such as styrene production. This study aims to use X-ray emissions to probe the dynamic behavior of the potassium-doped iron oxide catalyst, providing insights into hydrogen localization, binding energy, and catalyst activation, which are key to optimizing catalytic performance.

In this study, we aim to deepen our understanding of the radiation phenomena reported from HRM by employing a state-of-the-art Timepix3 detector, equipped with a Cadmium Telluride (CdTe) 1 mm scintillation crystal. This type of Timepix3 detector is expected to image both low-energy X-rays and higher energy gammas, making it an ideal instrument for investigating the complex radiation signatures of HRM. By analyzing these signatures, we seek to elucidate the catalysts' role in facilitating HRM formation and its

implication for hydrogenation reactions, offering a new perspective on catalyst design and efficiency.

Our experimental setup involves a stainless steel ultra-high vacuum (UHV) chamber that houses HRM source containing a potassium-doped iron oxide catalyst. Hydrogen or deuterium gas is flowed through this source and then chamber. Here, "catalyst activation" refers to the process by which the potassium-doped iron oxide catalyst reached an optimal state for HRM formation through prolonged hydrogen exposure at elevated temperatures (110–180 °C) and vacuum pumping operations.

By using the imaging Timepix3 detector we seek to provide a comprehensive analysis of the X-ray emissions from HRM for the following two situations: 1. Spontaneous emission case with only catalyst activation. 2. Activation with help of additional prior laser-excitation on the catalyst.

To ensure the accuracy of our measurements, we calibrated the Timepix3 detector using standard radioactive sources, such as Cs-137 and a Rb 21 keV XRF X-ray source. This calibration process is crucial for establishing a reliable baseline for detecting and interpreting the radiation emissions from HRM.

Our findings reveal a prominent peak in the energy spectra within the 25–50 keV range. Additionally, attenuation experiments with aluminum foil filters have uncovered a complex energy distribution, including a significant peak at 406 keV. These results offer valuable insights into the radiation behavior of hydrogen-loaded materials and challenge previous assumptions about the nature of emissions from HRM.

By enhancing our current understanding of HRM radiation, this study paves the way for future research and potential applications in various scientific and industrial domains. The use of advanced detection technology, such as the Timepix3 detector, underscores the importance of precision and accuracy in investigating the intricate radiation phenomena associated with hydrogen-rich systems. Specifically, the methodology developed here can be applied to other catalysts, providing a novel tool to study hydrogen-catalyst interactions in reactions like ammonia synthesis or hydrocarbon reforming, where hydrogen plays a critical role.

Despite extensive studies on HRM, the specific mechanisms underlying its X-ray emissions, particularly in the context of hydrogen-loaded catalysts, remain poorly understood. This study aims to bridge this knowledge gap by leveraging the advanced capabilities of the Timepix3 detector, offering unprecedented precision in capturing these emissions.

2. Results

After careful calibration of the Timepix3 detector (see Sections 4.3 and 4.4) using both the 21 keV X-ray source and the Cs137 source, the detector was positioned at a distance of 20 cm from the Hydrogen Rydberg Matter (HRM) chamber. The purpose of this positioning was to capture the X-ray emissions generated by the HRM source under nonactivated and spountaneous emission state.

2.1. X-Ray Spectra from HRM Using Timepix3 Energy

In Figure 1 we can see the two different spectra state measured with the Timepix detector, the red spectrum with low activity is the normal background in the laboratory.

In Figure 1 the energy spectra displayed a significant increase in the 25–50 keV range, and also in the higher energy range up to 1.0 MeV.

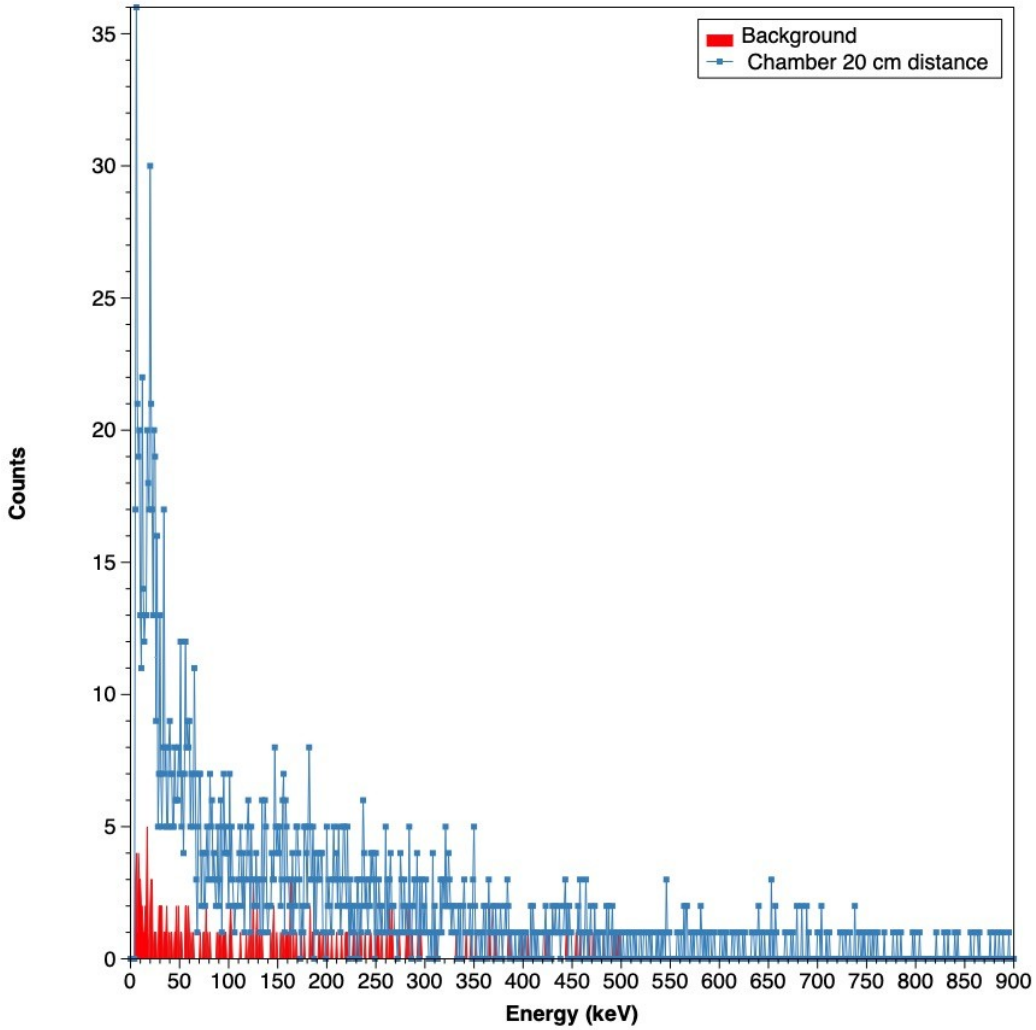


Figure 1. Comparison of background radiation (red) and HRM activated X-ray emissions (blue), highlighting the increased activity in the 25–50 keV range.

2.2. Radiation Picture Before Pumping at 1 m Distance from Chamber

To further visualise the X-ray emissions, radiation images were taken before and after the HRM source was activated. These pictures were captured at a distance of 1 m from the chamber, providing a detailed view of the radiation intensity and distribution.

The baseline radiation, captured before the system was pumped with hydrogen, showed a relatively low level of X-ray activity, with 2651 active pixel hits and a cumulative pixel value of 112,931. In contrast, after the HRM source was activated and hydrogen was introduced into the system, there was a noticeable increase in X-ray activity. The radiation images showed 4240 active pixel hits, with the total pixel value rising to 190,812. This increase in activity strongly indicated that the HRM source was generating X-rays as expected (see Figure 2 below), confirming the effectiveness of the experimental setup.

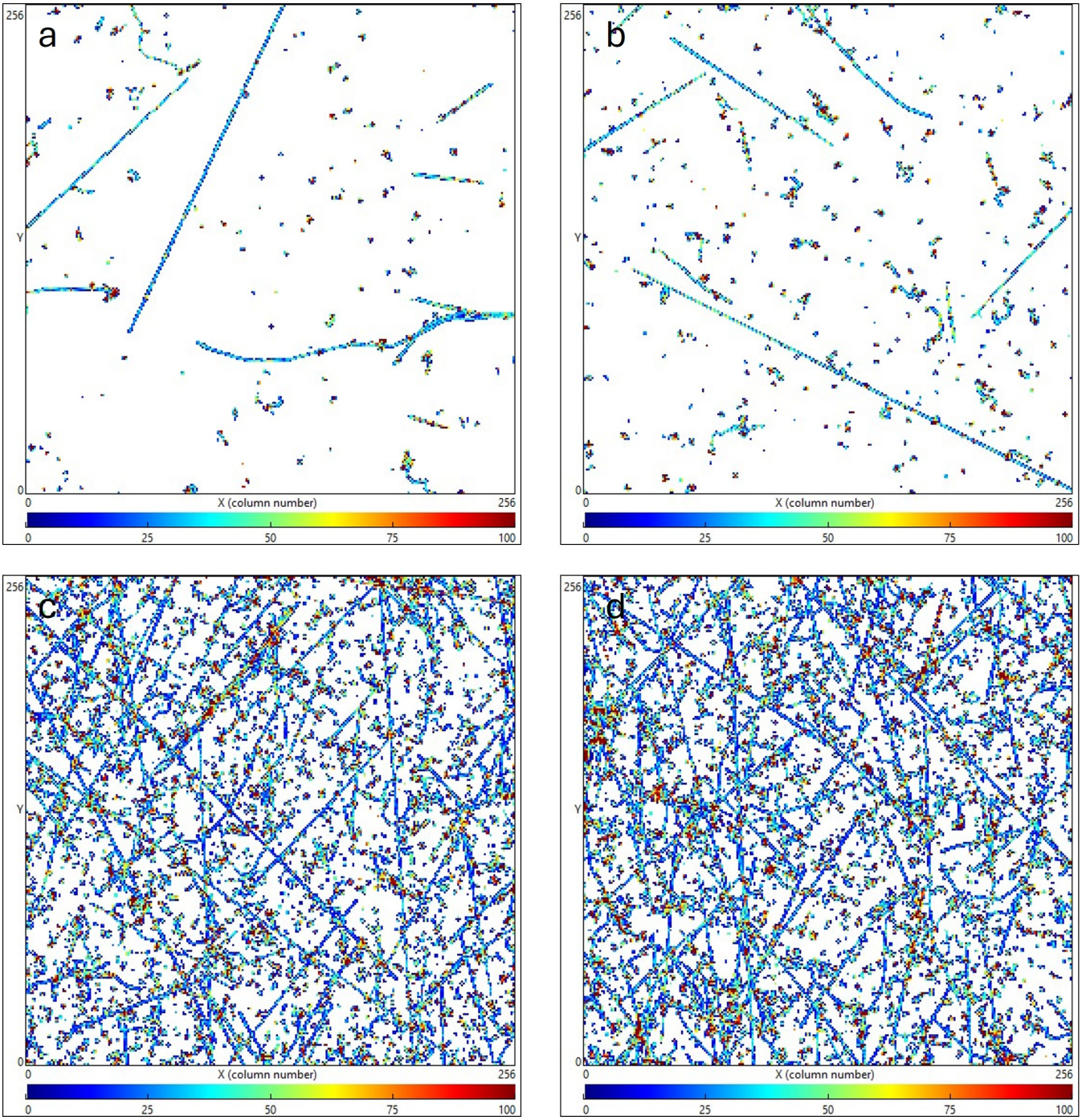


Figure 2. Radiation intensity before and after HRM activation X. The image captured at 1-m distance shows a significant increase in X-ray emission post-HRM activation, confirming the successful induction of X-ray activity in the system; (**a**) background radiation at 11:24 27 August showing 2651 active pixel hits with a sum of all pixel values 112,931, (**b**) 14:42 27 August showing 4240 active pixel hits with a sum of all pixels 190,812, (**c**) 14:23 30 August showing 26,366 active pixel counts with a sum of all pixels 1,038,140, (**d**) 20:49 30 August showing 28,420 active pixel counts with a sum of all pixels 1,138,070. These times indicate the exact moments of measurement on the specified dates, which are relevant for tracking the temporal evolution of the HRM activation process.

2.3. Energy of Discrete Emission X-Ray Events at Detector

The Timepix3 detector measured X-ray energies from the HRM source, revealing distinct peaks as shown in Figure 3. X-ray energy from Figure 3b showing 382 keV at the

detector, Figure 3d X-ray energy showing 487 keV at the detector. The 406 keV peak, a key finding of this study, is observed in subsequent attenuation experiments (see Figures 4–7).

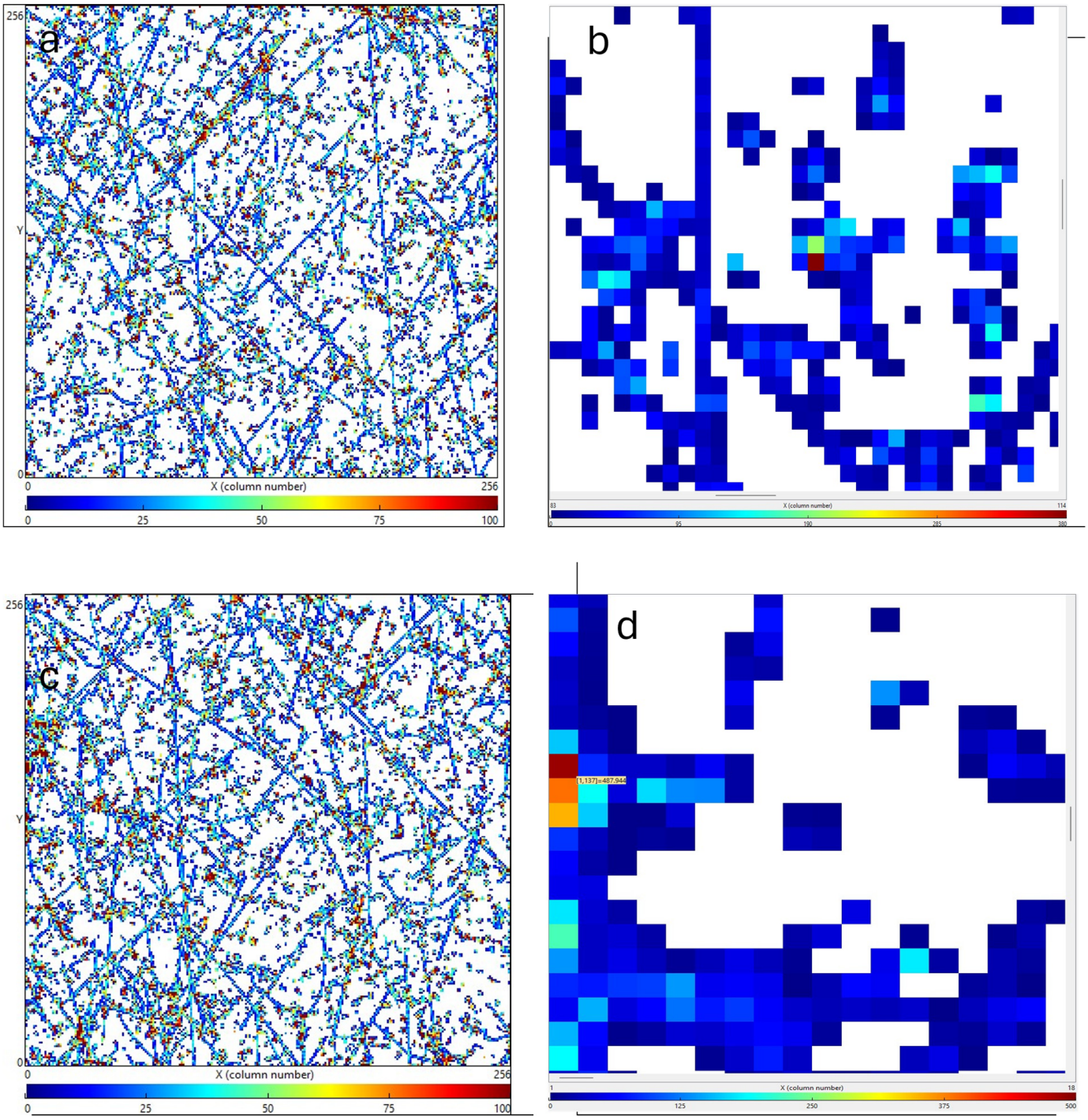


Figure 3. X-ray energy from (**a**) X-ray image from HRM reactor, (**b**) X-ray energy showing 190 keV at the detector. (**c**) X-ray image after continuous pumping (**d**) X-ray energy showing 487 keV at the detector. The 487 keV event, a key finding of this study, is observed in subsequent attenuation experiments.

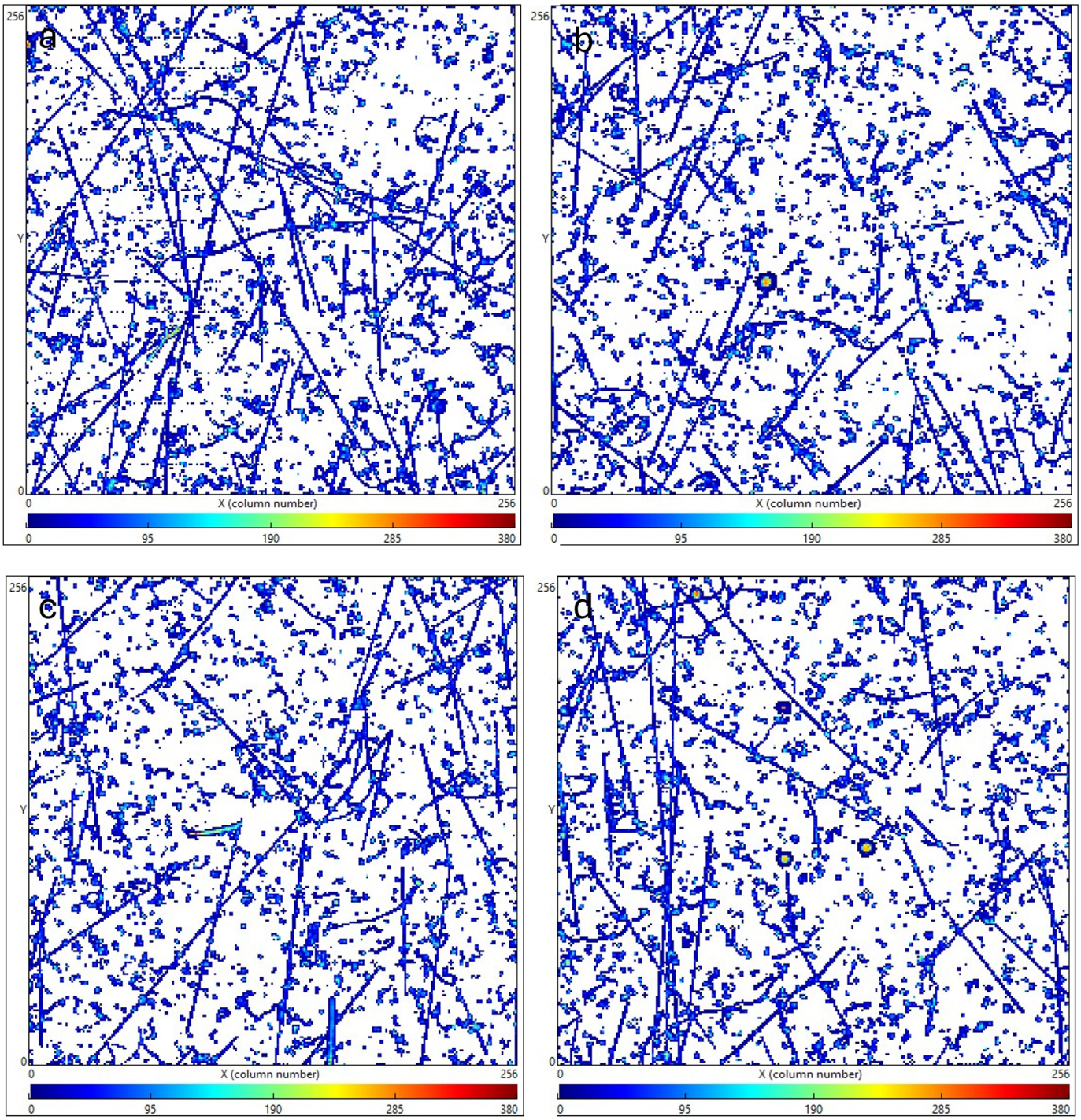


Figure 4. Timepix3 measurements using different absorption elements, spectra time 500 s, energy discriminated between 50 and 400 keV: (**a**) 2 m Ir foil max 345 keV pixel 19,447 total 702,087, (**b**) 2 m Zn foil 368 keV pixel 17,466 total 637,117, (**c**) 2 m Cu foil 318 keV pixel 17,728 total 659,926, (**d**) 2 m Ta foil 365 keV pixel 17,996 total 672,266.

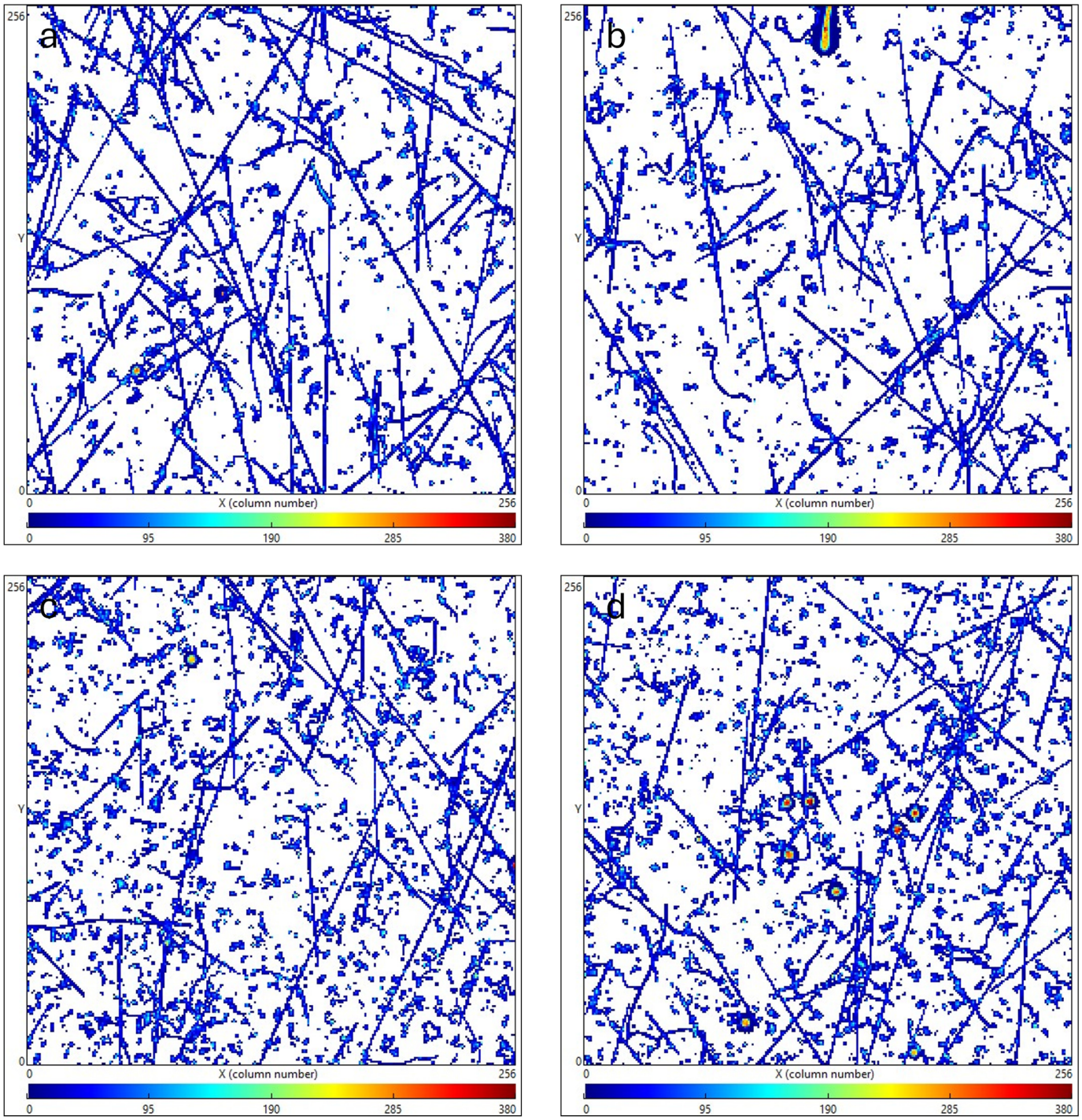


Figure 5. X-ray attenuation with aluminium, (**a**) home one al layer max 330 keV pixel 16,906 total 546,335, (**b**) home four layers max 372 keV pixel count 14,157 total 457,783, (**c**) lab 2 m one al layer max 362 keV pixel count 17,863 total 643,888, (**d**) lab 1 m four al layers max 411 keV pixel count 18,366 total 682,026, lab 2 m four al layers max 486 keV pixel count 19,706 total 725,888. The 406 keV peak is observed in panel (**d**), indicating a significant high-energy emission after attenuation with four aluminum layers at 1 m distance.

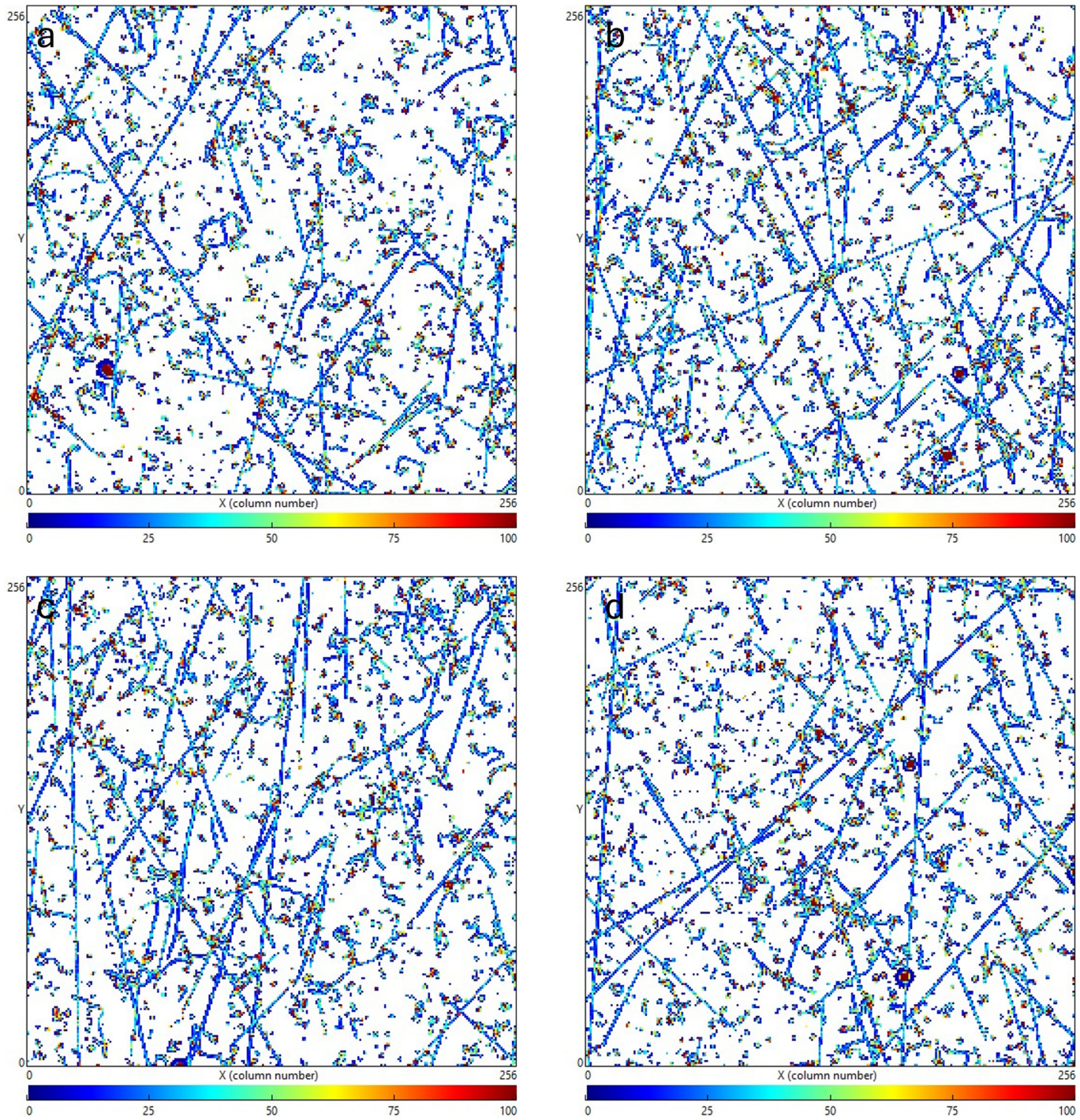


Figure 6. Timepix3 measurements. (**a**) 5 mm Al attenuation max 536 keV pixel count 16,182 total 579,744, (**b**) 5 mm Al 428 max pixel count 18,942 total 674,215, (**c**) 50 Al max 398 keV pixel count 17,829 total 632,588, (**d**) 100 mm Al max 563 keV pixel count 16,793 total 591,839. The 406 keV peak is also evident in panel (**c**), confirming its presence across different attenuation thicknesses.

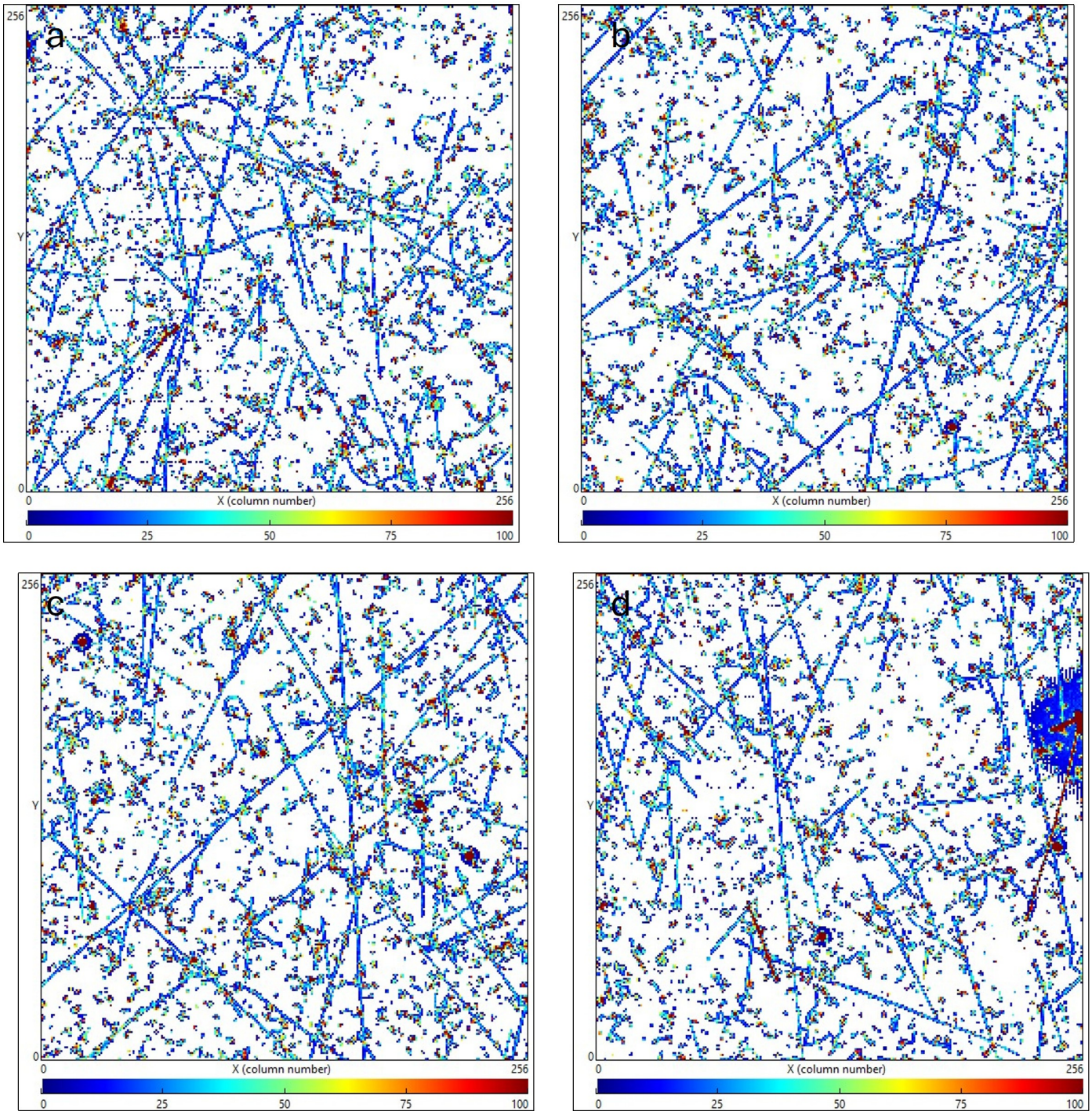


Figure 7. Timepix3 measurements. (**a**) Ir foil max 345 keV pixel 19,447 total 19,447, (**b**) Ir foil max 706 keV pixel count 19,056 total 697,781, (**c**) max 356 keV pixel 19,836 total 744,430, (**d**) Ir foil max 646 keV pixel 18,873 total 690,714.

2.4. Attenuation of X-Rays Through Aluminium Foil—Radiation Picture with 1 Al and Four Layers in Front of Detector at 2 m Distance from Chamber

To further research the energy of the X-rays being emitted from a potassium-doped iron oxide catalyst, we attenuated materials between the reactor and the X-ray detector.

2.5. Energy of X-Rays at Detector with Attenuation

Figure 5 below we can see the detectors response when adding attenuation layers of aluminum.

In the next Figure 6 below we attach thicker aluminum attenuation targets.

The aluminum attenuation target was then changed to Iridium foil as seen in Figure 7. below

As we can see from Figure 7d, we detect a heavy ion. A Timepix SiPIN detector, particularly when used with a thin foil (such as aluminum or iridium), can detect a variety of heavy ions. The foil in front of the detector serves to filter or degrade the incoming ions, affecting which ions can be detected and their energy.

Heavy Ions Detectable: Protons (H+).

Typically used as a light, thin barrier that may reduce the energy of incoming ions but does not significantly stop them. It is more suitable for lighter ions like protons or helium, allowing their detection while filtering out lower-energy electrons or photons. Iridium Foil.

Being much denser, iridium can significantly attenuate the energy of incoming ions, making it more suitable for detecting very heavy ions, or it can act as a target to generate secondary ions or other particles that can be detected by the Timepix SiPIN detector.

3. Discussion

In the analysis of the X-ray emissions, the results indicate that the HRM source emits X-rays predominantly in the 25–50 keV range, which aligns with the characteristics of spontaneous X-ray emissions from hydrogen-loaded materials. The prominent peak in this range suggests that the HRM source generates X-rays through a mechanism that involves electronic transitions or interactions within the hydrogen-loaded catalysts. From a catalyst perspective, this peak likely reflects changes in the electronic structure of the potassium-doped iron oxide catalyst as hydrogen s absorbed, providing insights into hydrogen localization and binding energy, which are critical for optimizing hydrogenation reactions like those in styrene production.

The high-energy event at 406 keV, observed through aluminum foil attenuation experiments, is particularly intriguing. This peak implies the presence of a secondary emission process that produces high-energy X-rays. One possible explanation is that these high-energy X-rays result from bremsstrahlung radiation, where electrons decelerate rapidly upon interacting with the dense material of the catalyst, or from secondary emissions triggered by initial X-ray interactions within the material. These high-energy emissions may indicate deeper interactions between hydrogen and the catalyst, potentially affecting its catalytic activity by altering hydrogen binding strength, which could be leveraged to design more efficient catalysts for industrial applications.

Implications for Catalyst Behavior. The differentiation between laser-induced and spontaneous activation of X-ray emissions provides significant insights into the radiation behavior of HRM. Laser-induced emissions, characterized by rapid particle bursts, suggest a direct correlation between the laser excitation and the emission of high-energy particles. In contrast, the spontaneous emissions, which occur post-activation, highlight the inherent radiative properties of the potassium-doped iron oxide catalyst when hydrogen or deuterium is introduced. These spontaneous emissions may reflect the catalysts ability to sustain HRM formation, a property that is crucial for its performance catalytic processes, offering a new method to study catalyst stability, and activation under reaction conditions.

The attenuation experiments further underscore the observation of the emitted X-rays, revealing a broad spectrum of energies. The observed energy distribution is consistent with a multi-faceted mechanism within the HRM source, where different processes contribute to the overall emission profile. This complexity suggests that the catalyst undergoes dynamic changes during hydrogenation, which can be probed using X-ray emission spectroscopy to understand catalyst behaviour in real-time without disturbing the process, a technique that could be applied to other catalytic systems.

Comparison with similar X-ray experiments. The observed X-ray emissions from the HRM system show notable similarities to X-ray emissions detected in other hydrogen-loaded metal systems. For instance, the Karabut experiment involving deuterium-loaded palladium under electrical excitation reported X-ray emissions in the 1.5 to 20 keV range [3]. These emissions, like those observed in this study, display distinct energy peaks and are correlated with specific experimental conditions.

In both cases, the X-ray emissions are not easily explained by conventional radiation sources or known physical processes at such low energies. The presence of high-energy X-ray 406 keV event observed in this study, further suggests that secondary excitation processes or interactions within the material might play a crucial role. For example, by understanding how hydrogen absorption affects the electronic structure environment of the catalyst, we can design materials with tailored properties for hydrogenation, such as enhanced efficiency in styrene production. The identification of a high-energy event at 406 keV opens new avenues for understanding the emission processes in hydrogen-rich systems. This finding could have significant implications for the development of advanced materials, particularly in fields where hydrogenation reactions play a crucial role. The distinct energy distributions observed may also influence future research on catalyst design, potentially leading to more efficient industrial processes or novel applications in radiation detection technologies.

The detection of X-rays in similar energy ranges and the correlation with hydrogen or deuterium interactions point to underlying mechanisms that may be common across different experiments. These findings indicate that the radiation phenomena observed in HRM could be part of a broader class of radiation emissions from hydrogen-loaded systems. While the absence of muonic X-ray peaks challenges previous hypotheses [1], it underscores the necessity for further investigation into the exact mechanisms driving these emissions. Future studies could explore the role of different catalyst compositions or hydrogen isotopes in modifying the X-ray emission spectra.

Technological and Theoretical Implications. These findings challenge previous hypotheses that primarily attributed the emissions from HRM to muons. The absence of expected muonic X-ray peaks at specific energies, such as 346.8 keV, upon aluminum attenuation, suggests that the emissions are predominantly of a classic X-ray nature. This necessitates a reevaluation of the current understanding of the emission mechanisms in hydrogen-loaded materials.

Moreover, the successful deployment of the Timepix3 detector highlights its efficacy in distinguishing between different types of radiation and capturing detailed energy spectra. This capability is crucial for advancing research in hydrogen-rich systems and provides a robust tool for future studies.

The 25 keV to 50 keV peak aligns with spontaneous X-ray emissions from hydrogen-loaded catalysts, likely due to electronic transitions in the HRM, offering insights into how hydrogen affects the catalysts electronic structure. The 406 keV peak suggests secondary processes such as bremsstrahlung or nuclear interaction, which could indicate unique catalytic properties under extreme conditions, warranting further investigation with deuterium variants to enhance catalytic performance.

Compared to Karabut's deuterium-palladium experiments (1.5 keV to 20 keV X-rays) [3], HRM emissions extend to higher energies, indicating unique catalyst dynamics. The absence of muonic peaks (e.g., 346.8 keV) refutes prior hypotheses [1], favoring a classic X-ray profile. The heavy ion-like event in iridium foil data, resembling pion-like tracks per Bergmann et al. [4], hints at possible nuclear reactions, warranting investigation with deuterium variants.

These findings underscore the Timepix3's precision in radiation studies and suggest HRM's potential in catalysis and energy applications, building on recent macroscopic HRM research [5].

Recent studies on HRM have explored its potential in energy storage and conversion, where the interaction between hydrogen and metal catalysts under extreme conditions plays a critical role [5]. These studies, however, have primarily focused on the macroscopic properties of HRM, with less attention given to the micro-level radiation phenomena that may underlie these processes. By addressing this gap, the current research contributes to a more comprehensive understanding of HRM and its potential technological applications.

4. Materials and Methods

4.1. Experimental Setup

The experimental setup for Hydrogen Rydberg Matter (HRM) detection is depicted in Figure 8. The reactor, which houses the HRM catalyst, is coupled with a CdTe-based Timepix3 X-ray detector (Advacam, Praha, Czech Republic). This arrangement is specifically designed to capture and analyze the X-ray emissions originating from the HRM reactor (Kimball Physics, Wilton, NH, USA).

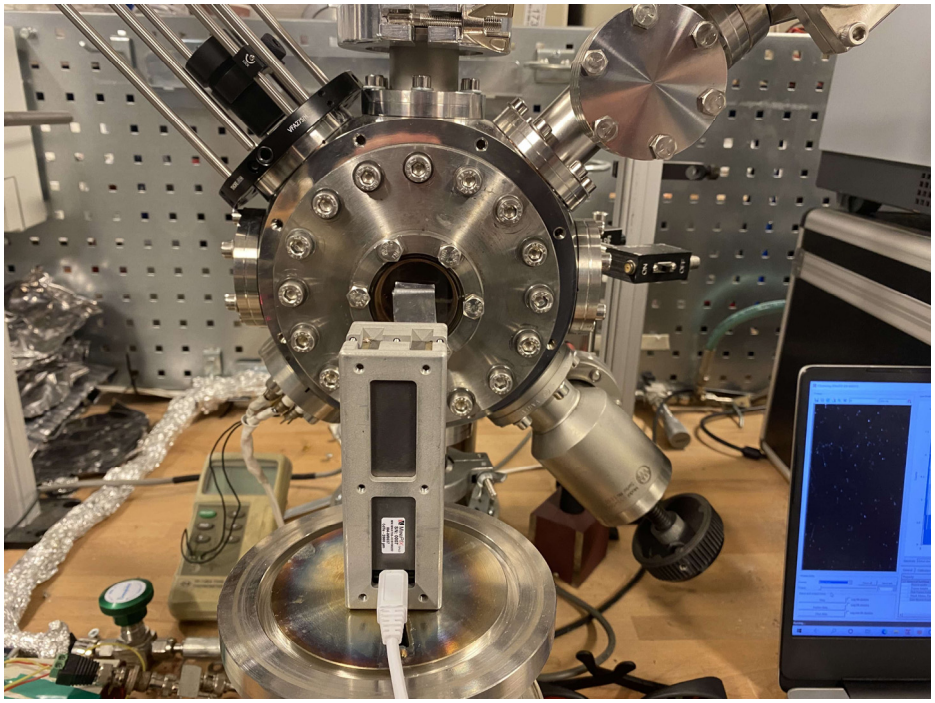


Figure 8. Picture of the experimental reactor for obtaining radiation from Hydrogen Rydberg Matter and the CdTe Timepix3.

The experimental configuration, illustrated in Figure 8, integrates several critical components designed to maintain ultra-high vacuum (UHV) conditions and precise control over experimental parameters.

The experimental setup for investigating X-ray emissions from Hydrogen Rydberg Matter (HRM) involves a sophisticated assembly designed to maintain ultra-high vacuum (UHV) conditions and precise control over the experimental parameters. The core component is a 6-inch spherical octagon UHV chamber fabricated from stainless steel 304 L, sourced from Kimball Physics (Wilton, NH, USA). This chamber is essential for minimizing contamination and ensuring a controlled environment for the experiments.

The HRM source (See Figure 9 below) comprises a solid block of stainless steel 321, engineered with perforated holes to house the Rydberg state catalysts. These catalysts are critical for the HRM formation and are composed of iron oxide doped with potassium (Fe_2O_3), known for its efficacy in facilitating hydrogenation reactions. The stainless steel 321 used here is an alloy with a nominal composition of approximately 17–19% chromium, 9–12% nickel, 2% manganese, 0.08% carbon, and trace amounts of titanium (up to 0.7%), with the balance being iron, ensuring high purity (99.999% relative to non-metallic impurities) for the experimental components. The HRM source is surrounded by an ATEX certified high-temperature band heater that maintains the operating temperature between 110–180 °C, essential for catalyst activation and maintaining the desired reaction conditions.

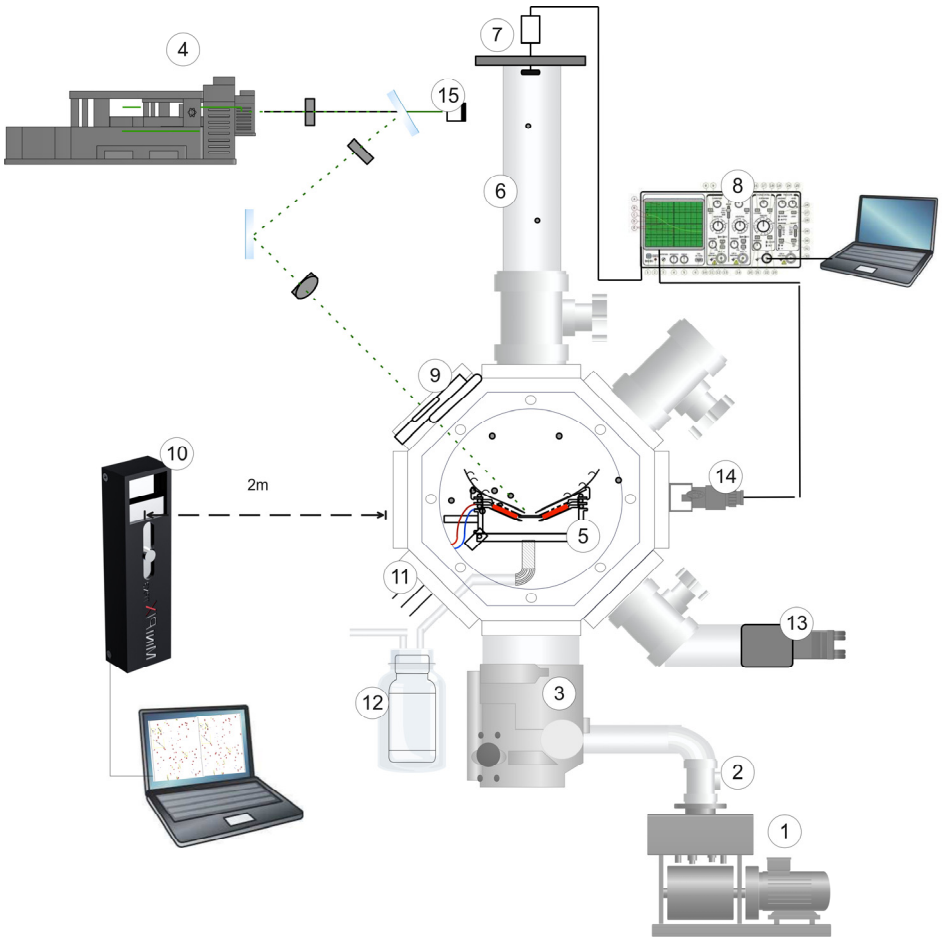


Figure 9. Schematic of the experimental setup showing the UHV chamber, the Timepix3 detector, and the YAG laser used for inducing X-ray emissions in HRM; 2 beam Q switched YAG laser (4), UHV chamber, turbo molecular pump (3), roughing pump (1), oil trap (2) Time-Of-Flight tube (6), Faraday cup detector (7), ns laser diode (14), Beam alignment (15), XYZ motion manipulation, laser view-port lens (9), ultra-fast laser diode (13), Oscilloscope (8), Hydrogen bottle (11), Cold trap (12), gas feed-through flange (11), Hydrogen Rydberg Matter catalyst (5), pressure sensor (13), laser target, CdTe photon-counting radiation detector (10).

Hydrogen 99.999% purity or deuterium gas is introduced into the chamber through a precise needle valve, maintaining a steady gas pressure in the range of 10^{-4} to 10^{-7} mbar.

This setup is supported by an Edwards E2M28 Rotary Vacuum Pump (Edwards Vacuum, West Sussex, UK) and a TMU 261 turbo molecular pump (Pfeiffer Vacuum, Asslar, Germany), which collectively achieve the necessary base pressure for the experiments. The hydrogenation process involves flowing the heated gas through the catalysts, and the initial

activation can take several weeks due to the requirement for extensive interaction between the catalysts, target, and gas.

To induce additional emissions, a pulsed YAG laser operating at 1064 nm with a maximum pulse energy of 500 mJ and a 5-ns pulse duration is employed. The laser beam is precisely focused above a metal target in the chamber using a short-pass dichroic spherical lens with an f = 270 mm focal length. The beam alignment is achieved using mirrors mounted on three-axes stages, ensuring optimal positioning during the experiments. The metal target, constructed from 99.999% pure stainless steel 321, is also mounted on an XYZ motion manipulator to accurately control its position.

Temperature control during the experiments is achieved using Pt-100 sensors (Cambell Scientific, Logan, UT, USA) attached to the laser target and the catalyst holder, providing real-time monitoring and feedback. The chamber components are meticulously cleaned using the methods described by Taborelli et al. [6] to remove surface contaminants such as silicon and oxide, which could hinder the activation process.

Timepix3 has been thoroughly evaluated with a variety of radiation and tracking sources [7], and is anticipated to give a more precise understanding of the radiation from materials containing hydrogen.

4.2. The Timepix3 USB Detector and Camera

The core detection apparatus for this study is the Advacam MINIPIX X-ray camera (Prague, Czech Republic), which integrates a single Timepix3 chip sensor. Developed by the CERN Medipix3 Collaboration (Geneva, Switzerland), the Timepix3 chip represents a significant advancement in pixel detector technology. It comprises a 256 $\times$ 256 pixel matrix, with each pixel measuring 55 μm, facilitating the high-resolution detection of ionizing particles. The Timepix3 chip, developed by the CERN Medipix3 Collaboration [7], comprises a 256 $\times$ 256 pixel matrix [8]. Its operational modes enable precise radiation measurement [9], with documented heavy ion tracking [10]. Its capability for 3D track reconstruction enhances its suitability for detecting complex radiation signatures [4].

The sensor coupled with the Timepix3 chip is composed of Cadmium Telluride (CdTe), selected for its high atomic number, density, wide energy band gap, and excellent resistivity, making it particularly suitable for room-temperature X-ray detection. The CdTe sensor is protected by a 500-nm thick aluminum layer, designed to minimize light-induced leakage currents, and operates under a bias voltage of -500 volts.

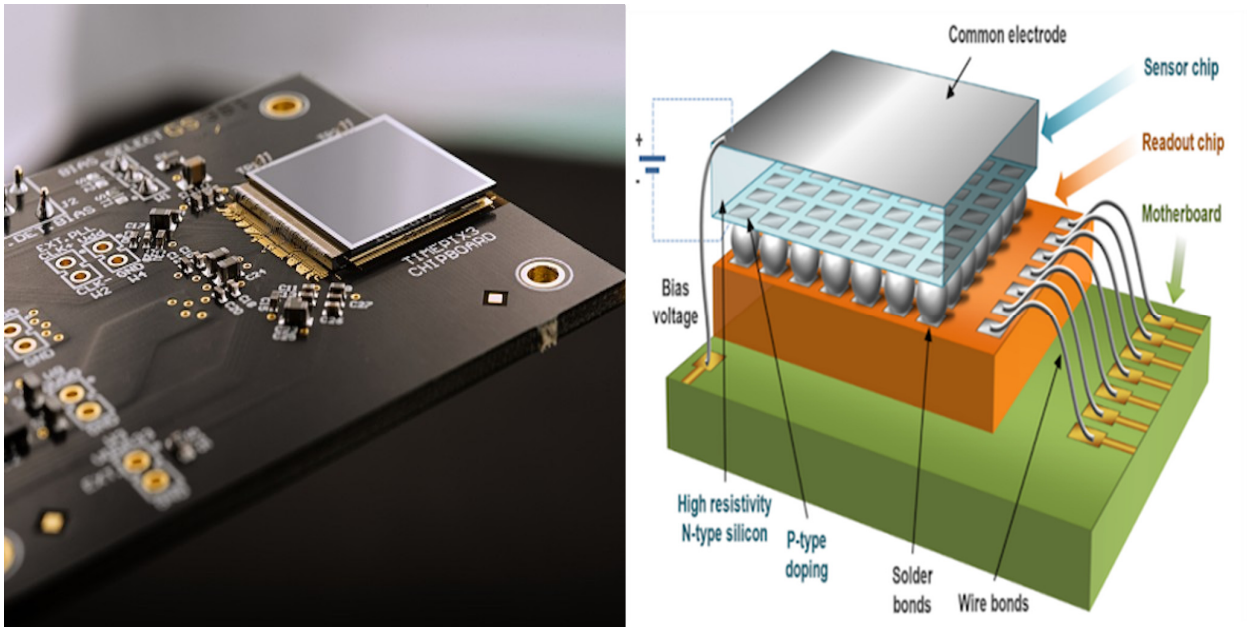
Functionally, the Timepix3 chip features three operational modes: counting, time of arrival (ToA), and time over threshold (ToT). These modes allow for precise measurement and categorization of different radiation types, including X-rays, electrons, neutrons, and alpha particles. The chip's sensitive area spans 14 mm by 14 mm, providing an energy resolution of 0.8 keV (Threshold Level, THL) and 2 keV (ToT), and it is capable of detecting X-rays with a minimum energy of 5 keV.

For data acquisition and analysis, the robust Pixet Pro software 1.7 from Advacam is employed. This software is integral for processing the data captured by the Timepix3 detector, ensuring accurate and reliable results. The detector underwent thorough calibration using standard radioactive sources such as Cs137 (662 keV) and a 21 keV X-ray source, confirming its linear response and reliability in measuring energy spectra.

The detailed calibration process involved positioning the detector at a fixed distance from the radioactive sources and acquiring ToT data to establish a relationship between ToT values and deposited energy. This calibration was crucial for ensuring the accuracy of the energy measurements obtained during the HRM experiments.

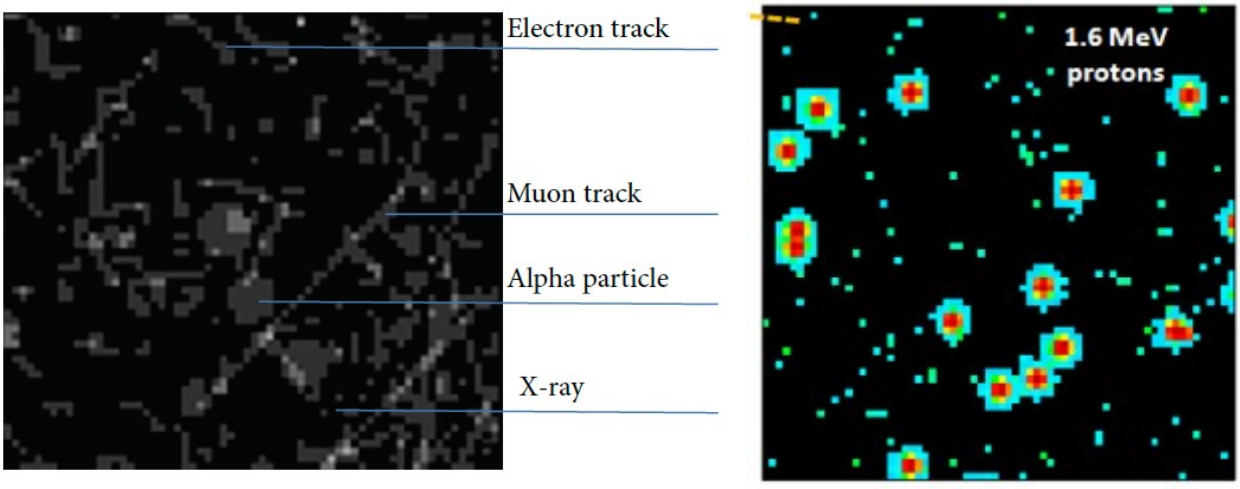
Presented in below is the Timepix3 detector response from differently charged particles. The different tracks from Electrons, Muons, Alphas, Protons, and X-rays can be seen clearly in the picture.

The Timepix3 detector's response to different radiation types, as shown in Figure 10, validates its suitability for detecting HRM emissions. Further illustrations in Figures 11–13 showcase its capability to distinguish among various charged particles and X-rays, thus validating its suitability for this study.



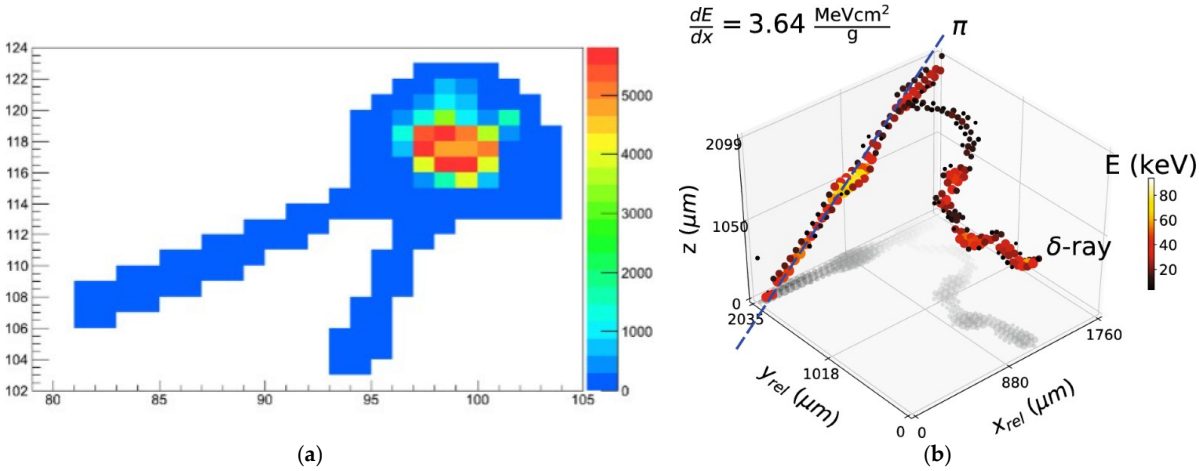
(**a**) (**b**)

Figure 10. Timepix3 detector [7,8], (**a**) picture of sensor, (**b**) schematic of sensor.



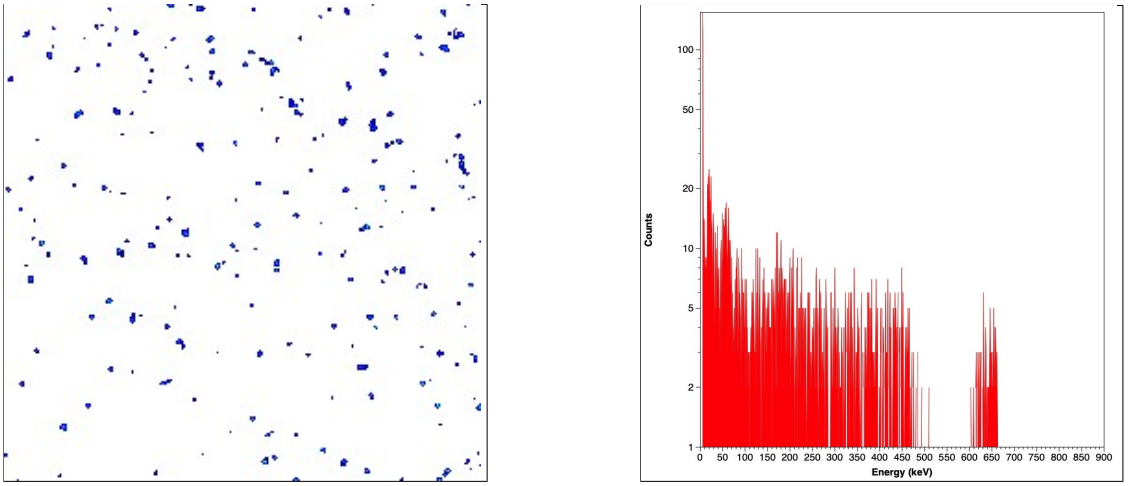
(**a**) (**b**)

Figure 11. Timepix3 detector response to (**a**) electrons, Muons, X-ray, Alphas; (**b**) Protons [9].



(**a**) (**b**)

Figure 12. Timepix3 detector response to (**a**) Interaction with one primary and fragments similar to delta-ray [10]; (**b**) Pion delta event [4]. In Figure 5a, particles were identified based on their track shapes and energy deposition patterns in the Timepix3 detector: electrons show thin, curly tracks; Muons exhibit long, straight tracks; X-rays appear as small, localized clusters; and alphas produce short, thick tracks due to their high energy deposition. In Figure 5b we can see a heavy ion energy deposition in the detector, creating a similar delta event as a Pion delta stopping event as shown in Figure 12 above.



(**a**) (**b**)

Figure 13. Timepix3 clustering: (**a**) Cs-137 662 keV source 8 s 10 cm, (**b**) energy spectrum from one of the spots in the middle of picture.

Figure 11a,b illustrate the ability of the Timepix3 detector to capture detailed particle tracks, further validating its suitability for the HRM study.

This comprehensive setup, centered around the Timepix3 detector, provides the necessary precision and accuracy required to advance our understanding of X-ray emissions from Hydrogen Rydberg Matter. The detailed calibration and robust design ensure that the collected data are both reliable and meaningful, paving the way for significant scientific insights. In Figure 12 below we can see the detectors response to electrons, Muons, Alphas and Pion events.

4.3. Calibration of the Timepix3 Detector Using a Cs-137 Source

Accurate energy measurement is a critical component of the experiment, and the Timepix3 detector was carefully calibrated using a Cs-137 radioactive source to ensure this

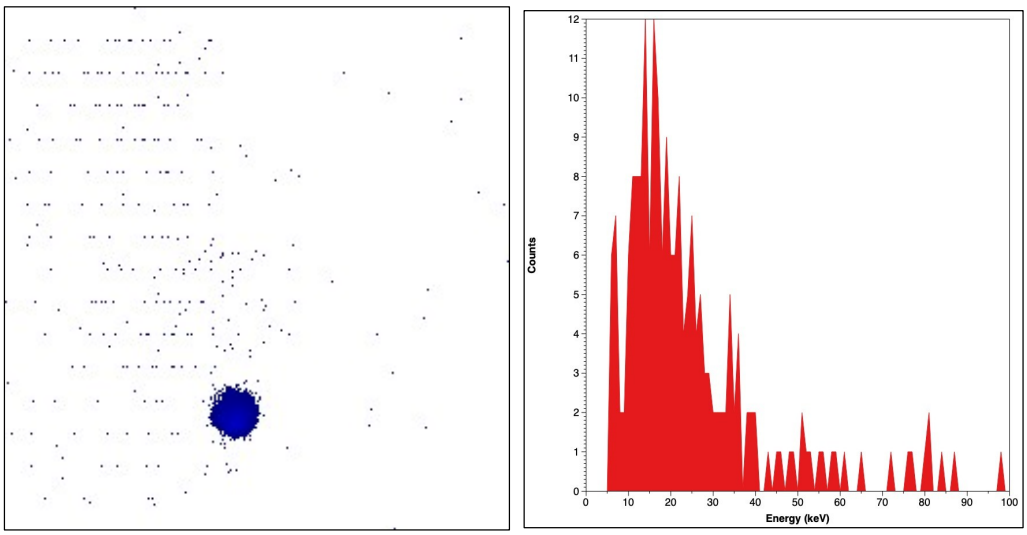
precision. Cs-137 is known for emitting gamma rays with a primary energy of 662 keV, which interacts with the Timepix3 sensor primarily through Compton scattering. In Figure 13 below we can see the Timepix respons to calibration target containing Cs-137.

The calibration source emits gamma rays with a primary energy of 662 keV, primarily interacting with the Timepix3 sensor through Compton scattering. The detector and the source were positioned at a fixed distance of 10 cm to maintain consistent geometry. As we can see in Figure 13a,b from this calibration, the energy peak of 662 keV is clear.

This calibration step was crucial for validating the detector's energy measurement capabilities. The clear identification of the Compton edge confirmed that the Timepix3 detector was accurately capturing and interpreting the energy levels of the incoming gamma rays, providing confidence in its ability to measure the X-ray emissions from the HRM source with high precision.

4.4. Calibration on the Timepix3 Using an 21 keV X-Ray Source

To complement the Cs137 calibration, the Timepix3 detector was also calibrated using a 21 keV X-ray source (seen in Figure 14). This calibration was particularly important for the detection of low-energy X-rays, which are a significant component of the emissions expected from the HRM source.



(**a**) (**b**)

Figure 14. Timepix3 measurements: (**a**) 21 keV X-ray spectrum using clustering, (**b**) picture of 21 keV X-ray source.

During the calibration process, the 21 keV X-rays interacted primarily with the silicon layer of the Timepix3 sensor through the photoelectric effect. This interaction is particularly significant for low-energy X-rays, as it results in the deposition of energy within the sensor that the detector can then measure. The detector was operated in Time-over-Threshold (ToT) mode, which measures the duration that the signal remains above a specific threshold, correlating directly with the energy deposited by each X-ray photon.

The data collected in ToT mode were analyzed to produce an energy spectrum, with the key indicator of successful calibration being a distinct peak at 21 keV. This peak confirmed that the Timepix3 detector was accurately tuned to detect low-energy X-rays, validating its suitability for the upcoming HRM experiments.

This calibration was instrumental in ensuring the reliability and accuracy of the Timepix3 detector, particularly in its ability to measure the low-energy X-rays expected from HRM emissions. The successful identification of the 21 keV peak demonstrated that the detector was

properly configured to capture the full range of X-ray energies, providing a solid foundation for the detailed analysis of radiation phenomena in Hydrogen Rydberg Matter.

5. Conclusions

This study not only confirms the presence of significant X-ray emissions from HRM but also identifies potential high-energy emission mechanisms that warrant further exploration. These emissions provide insights into the behavior of the potassium-doped iron oxide catalyst under hydrogenation conditions, revealing how hydrogen localizations and binding energy are influenced, which are critical for optimizing catalytic processes like styrene production. Future research could focus on varying the catalyst materials or introducing different isotopic hydrogen species to further elucidate the factors influencing X-ray production. Such studies could lead to the development of more efficient catalysts by tailoring hydrogen–catalyst interactions, directly addressing challenges in catalytic research. Additionally, the application of this research could extend to enhancing radiation detection technologies and improving our understanding of hydrogen-related radiation phenomena in both industrial and experimental settings.

This study demonstrates the exceptional capabilities of the Timepix3 detector in investigating X-ray emissions from Hydrogen Rydberg Matter (HRM). However, beyond the technical capabilities of the detector, the study offers a new perspective on catalyst behavior, showing how X-ray emission can be used to probe the electronic environment or the catalyst, providing a novel tool for catalyst characterization in hydrogen related reactions. The detailed energy spectra obtained reveal significant insights into the nature of these emissions, with a prominent peak in the 25–50 keV range and a notable high-energy peak at 406 keV. These findings enhance our current understanding of radiation phenomena in hydrogen-rich systems and challenge previous hypotheses regarding the nature of these emissions.

The results underscore the importance of precise calibration and rigorous experimental controls in the capture of accurate radiation profiles. The complex energy distribution observed through attenuation experiments with aluminum foil filters further highlights the multifaceted nature of the emissions from HRM. This complexity reflects dynamic changed in the catalyst during hydrogenation, offering a pathway to study catalyst activation and stability, which are central to improving catalytic performance in industrial applications.

Overall, this study provides a comprehensive analysis of the X-ray emission from HRM, paving the way for future research in this domain. The insights gained from this investigation have significant implications for the development of advanced materials and catalysis, as well as for the broader field of applied physics. Specifically, the findings can inform the design of advanced catalytic materials by leveraging the observed hydrogen catalyst interactions, potentially leading to more efficient hydrogenation processes, fine tuning reaction rates or contributing to the broader field of catalysis.

Author Contributions: Conceptualization, S.A.Z.-G. and S.O.; methodology, S.A.Z.-G.; software, S.A.Z.-G.; validation, S.A.Z.-G. and S.O.; formal analysis, S.A.Z.-G.; investigation, S.A.Z.-G.; resources, S.O.; data curation, S.A.Z.-G.; writing—original draft preparation, S.A.Z.-G.; writing—review and editing, S.O.; visualization, S.A.Z.-G.; supervision, S.O.; project administration, S.O.; funding acquisition, S.O. All authors have read and agreed to the published version of the manuscript.

Funding: This work was partially funded by the Norwegian Research Council under the Industrial Ph.D. program, Nordic Nuclear Energy Corporation AS, and Norrønt AS. The published results are part of a larger research and development project and were funded by Norway Grants (EEA and Norway Grants) (248497), Horizon 2020 Framework Program (H2020) project number (951974), NORNEC (Nordic Nuclear Energy Corporation), and NORRØNT AS. The support of the Icelandic Research Fund grant 217577-051 is acknowledged. The APC was funded by the University of Iceland.

Data Availability Statement: Data supporting the reported results are available upon request from the corresponding author. No new data were created, and data sharing is subject to privacy and ethical restrictions.

Acknowledgments: The authors express special thanks to Jan Mráz at Advacam for assisting with the X-ray camera installation and calibration.

Conflicts of Interest: The authors declare no conflicts of interest. The funders had no role in the design of the study; in the collection, analyses, or interpretation of data; in the writing of the manuscript; or in the decision to publish the results.

References

1. Holmlid, L.; Olafsson, S. Spontaneous ejection of high-energy particles from ultra-dense deuterium D(0). *Int. J. Hydrogen Energy* **2015**, *40*, 10559–10567. [CrossRef]
2. Lipson, A.; Miley, G.; Roussetski, A.; Karabut, A. Strong Enhancement of Dd-Reaction Accompanied by X-Ray Generation in a Pulsed Low Voltage High-Current Deuterium Glow Discharge with a Titanium Cathode. *Condens. Matter Nucl. Sci.* **2005**, *4*, 635–656.
3. Bergman, S. Low-Energy Nuclear Reactions. November 2013. Available online: https://readingfeynman.org/2020/11/25/low-energy-nuclear-reactions/ (accessed on 15 April 2025).
4. Bergmann, B.; Burian, P.; Manek, P.; Pospisil, S. 3D reconstruction of particle tracks in a 2 mm thick CdTe hybrid pixel detector. *Eur. Phys. J. C* **2019**, *79*, 165. [CrossRef]
5. Hirscher, M.; Yartys, V.A. Materials for hydrogen storage: Current research trends and perspectives. *Chem. Commun.* **2010**, *46*, 2607–2618.
6. Taborelli, M. Cleaning and Surface Properties. *Tech. Rep.* **2020**, 321–340.
7. Timepix3 | Knowledge Transfer. Available online: https://kt.cern/technologies/timepix3 (accessed on 15 April 2025).
8. Campbell, M.; Alozy, J.; Ballabriga, R.; Egidos, N.; Fernandez, J.; Heijne, E.H.M.; Kremastiotis, I.; Llopart, X.; Sriskaran, V.; Tlustos, L. The Timepix Family of Pixel Detector Readout Chips. Available online: https://indico.cern.ch/event/895924/contributions/4020698/attachments/2119022/3565847/Vertex2020MC.pdf (accessed on 21 May 2025).
9. Granja, C.; Jakubek, J.; Polansky, S.; Zach, V.; Krist, P.; Chvatil, D.; Stursa, J.; Sommer, M.; Ploc, O.; Kodaira, S.; et al. Resolving power of pixel detector Timepix for wide-range electron, proton and ion detection. *Nucl. Instrum. Methods Phys. Res. Sect. A Accel. Spectrometers Detect. Assoc. Equip.* **2018**, *908*, 60–71. [CrossRef]
10. Hoang, S.; Vilalta, R.; Pinsky, L.; Kroupa, M.; Stoffle, N.; Idarraga, J. Data analysis of tracks of heavy ion particles in timepix detector. *J. Phys. Conf. Ser.* **2014**, *523*, 012026. [CrossRef]

Disclaimer/Publisher's Note: The statements, opinions and data contained in all publications are solely those of the individual author(s) and contributor(s) and not of MDPI and/or the editor(s). MDPI and/or the editor(s) disclaim responsibility for any injury to people or property resulting from any ideas, methods, instructions or products referred to in the content.